Research Article | Vol. 10, No. 11 / 1 November 2020 / Optical Materials Express 2973

Optical Materials EXPRESS

Deposition and characterization of solution processed Se-rich Ge-Se thin films with specular optical quality using multi-component solvent approach

STANISLAV SLANG,[1,*] KAREL PALKA,[1,2] JIRI JANCALEK,[1,2] MICHAL KURKA,[2] AND MIROSLAV VLCEK[1]

[1]Center of Materials and Nanotechnologies, Faculty of Chemical Technology, University of Pardubice, Studentska 95, Pardubice 53210, Czech Republic
[2]Department of General and Inorganic Chemistry, Faculty of Chemical Technology, University of Pardubice, Studentska 95, Pardubice 53210, Czech Republic
[*]stanislav.slang@upce.cz

Abstract: The $Ge_{25}Se_{75}$, $Ge_{20}Se_{80}$ and $Ge_{15}Se_{85}$ thin films were deposited in specular optical quality from n-propylamine - methanol solvent mixture by spin-coating technique. As-prepared solution processed thin films were thermally stabilized to reduce the content of organic solvent residuals and optical properties, surface topography, composition, structure and chemical resistance of prepared Ge-Se thin films were studied in dependence of annealing temperature. Suitable thermal stabilization temperatures were found for each studied chalcogenide glass composition with respect to maintaining of thin films' low surface roughness and targeted elemental composition. Stabilized thin films exhibited high refractive index, high chemical resistance, low surface roughness and structure close to source bulk glasses. The experiments proved that used n-propylamine - methanol solvent offered suitable way for preparation of high optical quality Ge-Se thin films by solution based deposition route.

1. Introduction

Chalcogenide glasses (ChGs) are semiconducting materials with high refractive index, wide IR transparency region, low phonon energy and high ion conductivity [1,2]. Their interesting properties make them unique in comparison with other commercially produced glasses and they have found many applications in optics, optoelectronics and photonics [1–4]. ChGs can be used in a form of bulk material (e.g. lenses, windows, fibers, etc. [1,2,5,6]) or as an amorphous thin film deposited on appropriate substrate (e.g. optical recording discs, diffractive optical elements, planar waveguides, high-resolution photoresists, etc. [7–11]). In principle, ChG thin films can be deposited from gaseous phase or from their solutions in volatile solvents. Although, the vapour based deposition techniques (such as thermal evaporation, laser ablation or sputtering [7–11]) are used more frequently and generally provide thin films of good optical quality, the solution based deposition route (based on spin-coating, spiral bar-coating, dip-coating or electrospray, etc. [12–17]) offers some significant advantages. Solution processing of ChG thin films is much simpler than vapour based deposition, which is reflected in low cost instrumentation. Preparation of thin films from solutions can be potentially up scaled due to well-developed commercial printing techniques. Solution based deposition route also provides a way for deposition of unstable materials or for preparation of composite materials where ChG can serve as suitable host medium (e.g. for doping with semiconductor luminescent nanoparticles [16,18]).

In the past, the sulphide based solution processed ChG thin films were the main focus of research due to their simplicity of preparation [12–20]. Especially the As-S thin films are relatively easy to prepare in high optical quality from aliphatic amines but the arsenic content can limit

#408327 https://doi.org/10.1364/OME.408327
Journal © 2020 Received 25 Aug 2020; revised 5 Oct 2020; accepted 16 Oct 2020; published 22 Oct 2020

Optical Materials EXPRESS

some of their potential practical applications. The need for tailoring of suitable physio-chemical properties drives solution-processing research further into other ChG systems, notably to yet not well-developed deposition of selenide based ChG thin films. Recently, the As-Se thin films were prepared in specular optical quality from amine-alcohol multicomponent solvent [21], which overcame notorious low solubility of selenides in frequently used aliphatic amines. However, the presence of arsenic can again be undesirable for some applications so the focus shifts to other selenide ChG systems. In the past, non-toxic thin films based on Ge-Se system were prepared from simple aliphatic amine or diamine solvents [22,23], but they proved to be difficult to deposit in good optical quality. A simple amine route resulted in thin films with significant undesirable surface roughness and the compositional uniformity was also questionable when precipitated particles and other phases were present in deposited thin films.

As demonstrated in [21,24], the selenium based ChGs (and especially with chalcogen overstoichiometry) need other solvent, which would help to disperse selenium-based ionic dissolution products. We offer an alternative route for preparation of Ge-Se thin films in high optical quality from binary n-propylamine - methanol solvent mixture. The three different Ge-Se ChGs ($Ge_{25}Se_{75}$, $Ge_{20}Se_{80}$ and $Ge_{15}Se_{85}$) were quantitatively dissolved in the proposed binary solvent and thin films were deposited with low surface roughness and in targeted elemental composition. The thermal treatment was used to reduce content of organic residuals and the effect of thermal stabilization on thin films properties was studied by various optical and structural analysis techniques.

2. Experimental details

Source bulk $Ge_{25}Se_{75}$, $Ge_{20}Se_{80}$ and $Ge_{15}Se_{85}$ chalcogenide glasses (ChGs) were synthetized by standard melt-quenching method. Pure 5N elements were weighted into clean quartz ampules in calculated amounts and sealed under vacuum (approx. 10^{-3} Pa). Loaded reagents were melted in a rocking tube furnace at 950 °C for 72 hours. The ampules with melted glasses were quenched in a cold water.

Synthetized Ge-Se ChGs were grinded inside agate bowl and weighted into glass vials to planned concentration 0.075 g of ChG powder per 1 mL of n-propylamine ($PrNH_2$) - methanol (MeOH) mixture solvent (10% vol. solution of MeOH in $PrNH_2$). The MeOH-$PrNH_2$ solvent was added inside nitrogen-filled glovebox (O_2, H_2O < 0.1 ppm) due to its high hygroscopicity. Glass vials were sealed and ChGs were dissolved under rigorous stirring using a magnetic stirrer. The ChGs were quantitatively dissolved after 24 hours and prepared solutions were clear without any precipitate or turbidity.

ChG thin films were deposited by spin-coating technique. The ChG solutions were pipetted onto rotating soda-lime substrates and spin-coated (spin-coater Laurell WS-650Mz-23NPPB) in protecting nitrogen atmosphere (O_2, H_2O < 0.1 ppm) at 2000 rpm for 60 s. Deposited thin films were soft baked by annealing at 60 °C on a hot plate for 20 min (hereafter referred to as as-prepared thin films). The as-prepared thin films were subsequently thermally stabilized (hard baked) up to 180 °C ($Ge_{15}Se_{85}$), 210 °C ($Ge_{20}Se_{80}$) and 240 °C ($Ge_{25}Se_{75}$), respectively, (hereafter referred as thermally stabilized thin films). The annealing temperatures were chosen with respect to T_g of studied ChG material and ongoing thermally-induced structural and compositional changes (see Section 3). Thermal stabilization process was again carried out inside a nitrogen-filled chamber to avoid undesirable oxidation or hydrolysis.

The transmission spectra of prepared Ge-Se thin films were measured by a UV-VIS-NIR spectrometer (Shimadzu UV3600 Plus) in the spectral range 190–2000 nm. The measurements were performed on eight samples for each Ge-Se ChG composition and individual treatment. The thickness and refractive index of studied thin films were determined by fitting procedure described in [25] based on the combination of Wemple-DiDomenico's equation [26] and Swanepoel's model of thin films on finite substrate [27]. The Tauc's method for semiconductors [28] was

Optical Materials EXPRESS

used for determination of optical bandgap. Examples of used fitting procedures are depicted in Fig. 1. Obtained values of thickness and optical parameters were averaged and presented error bars represent standard deviation from averaged values.

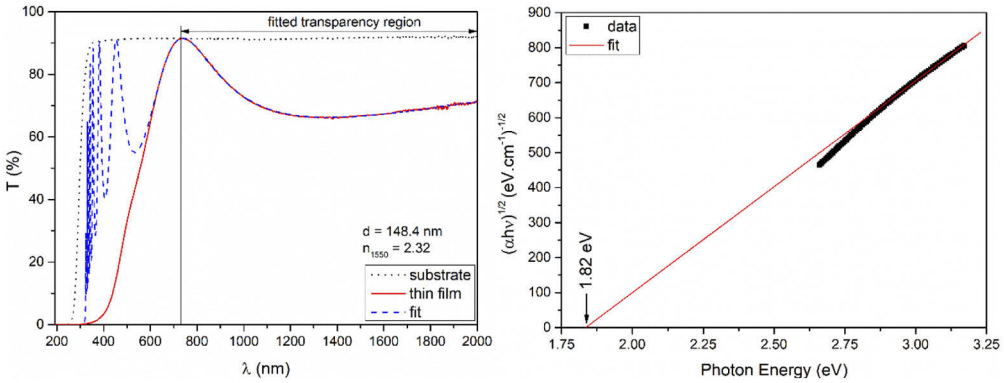

Fig. 1. Left: The example of transmission spectrum of spin-coated $Ge_{20}Se_{80}$ thin film annealed at 210 °C (red solid line) and soda-lime substrate (black dot line) together with fitted transmission spectrum (blue dash line). Right: Determination of optical bandgap of the same $Ge_{20}Se_{80}$ thin film according to Tauc's method.

Surface roughness of spin-coated Ge-Se thin films was studied by atomic force microscopy (AFM) in semicontact mode. Samples were measured by Solver Next (NT-MDT) microscope equipped with NSG10 tips (NT-MDT) on four 5×5 μm areas (two areas on two different samples for each individual composition and thermal treatment). The surface roughness was determined from AFM scans as a root mean square value (RMS) according to ISO 4287/1 norm. Error bars represent standard deviation of measured values.

The scanning electron microscopy (SEM) scans and elemental composition data were obtained using scanning electron microscope LYRA 3 (Tescan) equipped with EDS analyzer AZtec X-Max 20 (Oxford Instruments). The EDS measurements were performed at 5 kV acceleration voltage on ten 400×400 μm areas (five areas on two different samples for each individual composition and thermal treatment).

Structure of source bulk Ge-Se ChGs, deposited thin films and amorphous selenium was studied by MultiRAM (Bruker) FT-Raman spectrometer utilizing 1064 nm Nd:YAG laser excitation beam with 50 mW intensity (2 cm^{-1} resolution, 64 scans). Presented Raman spectra were normalized by the intensity of the most intensive band in each individual spectrum.

The FT-IR spectra of prepared Ge-Se thin films were measured by Vertex 70v FTIR spectrometer (Bruker) equipped with single-bounce diamond ATR crystal in 6000–30 cm^{-1} region (4 cm^{-1} resolution, 64 scans). The FT-IR spectra were normalized by the intensity of the soda-lime substrate band at approx. 916 cm^{-1}.

The wet etching technique was used to determine chemical resistance of spin-coated Ge-Se thin films. Samples were etched in 0.05 vol. % ethylenediamine (EDA) solution in dimethyl sulfoxide at 25 °C. Etching times and subsequently etching rates were evaluated by procedure described in [29].

3. Results and discussion

The source $Ge_{25}Se_{75}$, $Ge_{20}Se_{80}$ and $Ge_{15}Se_{85}$ ChGs were quantitatively dissolved in binary MeOH-$PrNH_2$ solvent and thin films were deposited in specular optical quality (examples of transmission spectra are given in Fig. 2). The Ge-Se solutions proved to be very sensitive to presence of oxygen and moisture (thermally stabilized thin films prepared in ambient condition

Optical Materials EXPRESS

contained up to 25 at. % of oxygen) so dissolution, deposition and annealing part of experiment was carried out in nitrogen filled glovebox.

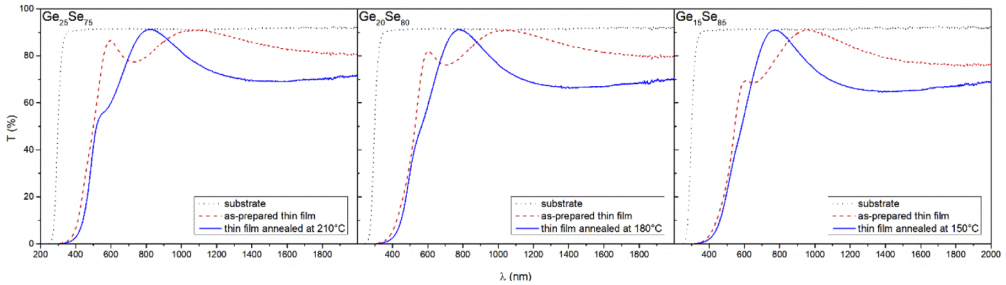

Fig. 2. The examples of transmission spectra of solution processed $Ge_{25}Se_{75}$, $Ge_{20}Se_{80}$ and $Ge_{15}Se_{85}$ thin films together with spectrum of used substrate.

At first, the as-prepared Ge-Se thin films were thermally stabilized (hard baked) up to temperatures slightly above the T_g of source bulk glass of the same composition (for $Ge_{25}Se_{75}$ T_g = 214-228 °C, for $Ge_{20}Se_{80}$ T_g = 154-159 °C and for $Ge_{15}Se_{85}$ T_g = 108-122 °C [30–33]). However, preliminary results proved that this approach is unsuitable for $Ge_{15}Se_{85}$ and $Ge_{20}Se_{80}$ solution processed thin films and they require higher temperatures (above their T_g) to achieve structural changes leading to stabilized glass material. Thus, the $Ge_{25}Se_{75}$ thin films were annealed up to 240 °C, $Ge_{20}Se_{80}$ thin films up to 210 °C and $Ge_{15}Se_{85}$ thin films up to 180 °C. The thickness, surface roughness, refractive index (at 1550 nm) and optical bandgap of the as-prepared and annealed solution processed Ge-Se thin films are summarized in Table 1 (thickness was rounded to one decimal digit, optical parameters to two decimal digits).

Thermal dependence of thickness (Fig. 3 - left) confirms that stabilization of Ge-Se solution processed thin films is connected with significant thickness contraction. It can be explained by release of a) occluded (chemically non-bonded) molecules of organic solvent residuals at lower temperatures and b) structural changes connected with release of chemically bonded solvent molecules at higher temperatures (primarily from ionic dissolution products containing bonded $PrNH_2$). Data shows that in case of Ge-Se solution processed thin films, the most significant thickness contraction occurs at temperatures up to 150 °C and after that, the thickness decrease is less pronounced (especially in case of $Ge_{25}Se_{75}$ thin films). The deposited thin films also get thinner with increasing content of selenium in dissolved bulk glass despite using the same mass concentration. As demonstrated in [21], the solution processed $As_{30}S_{70}$ thin films are thicker and contain more organic residuals than $As_{30}Se_{70}$ thin films. In case of germanium chalcogenides, the as-prepared $Ge_{25}S_{75}$ thin films deposited from less volatile n-butylamine solvent (the same ChG concentration) were still much thicker (396 nm [34]) than our as-prepared $Ge_{25}Se_{75}$ thin films (289 nm, Table 1.) deposited from more volatile MeOH-$PrNH_2$ solvent mixture. We can speculate that Ge-Se thin films get thinner with higher content of selenium due to combination of low selenium ability to hold on solvent organic molecules and possible different viscosity of used Ge-Se solutions. The surface roughness of as-prepared thin films (Fig. 3 - right) is very small (below 5 nm) and it does not influence films' specular quality. Moreover, surface roughness slightly decreases with an increasing annealing temperature and drops below 2 nm in the case of samples stabilized above 150 °C. It should be noted that opposite behaviour (increase of surface roughness with increasing annealing temperature) was observed on sulphide-based spin-coated ChG thin films [15,34] while arsenic-selenium-based thin films do not exhibit any significant thermally induce changes of their surface roughness (up to thin filmś degradation temperatures) [21]. This suggests that selenide-based solution processed ChG thin films have a better tendency

Optical Materials EXPRESS

Table 1. Values of $Ge_{25}Se_{75}$, $Ge_{20}Se_{80}$ and $Ge_{15}Se_{85}$ thin films' thickness, surface roughness, refractive index at 1550 nm (n_{1550}) and optical bandgap (E_g^{opt}).

$Ge_{25}Se_{75}$	Thickness (nm)	Roughness (nm)	n_{1550}	E_g^{opt} (eV)
as-prepared	289.3 ± 4.6	2.19 ± 0.38	1.90 ± 0.01	2.09 ± 0.01
T – 90 °C	253.0 ± 5.8	1.98 ± 0.19	2.01 ± 0.02	2.05 ± 0.01
T – 120 °C	225.7 ± 4.9	0.86 ± 0.05	2.11 ± 0.01	1.98 ± 0.01
T – 150 °C	187.0 ± 4.1	1.16 ± 0.08	2.24 ± 0.01	1.88 ± 0.01
T – 180 °C	192.1 ± 3.6	0.62 ± 0.26	2.22 ± 0.01	1.89 ± 0.01
T – 210 °C	181.1 ± 3.7	0.31 ± 0.03	2.24 ± 0.01	1.89 ± 0.01
T – 240 °C	166.7 ± 4.4	0.32 ± 0.02	2.24 ± 0.01	1.91 ± 0.01
$Ge_{20}Se_{80}$				
as-prepared	277.1 ± 5.8	2.90 ± 0.16	1.96 ± 0.01	2.03 ± 0.01
T – 90 °C	239.3 ± 5.7	1.68 ± 0.15	2.07 ± 0.01	1.96 ± 0.01
T – 120 °C	205.0 ± 5.8	2.30 ± 0.16	2.18 ± 0.02	1.85 ± 0.01
T – 150 °C	177.1 ± 3.7	1.45 ± 0.11	2.29 ± 0.01	1.80 ± 0.01
T – 180 °C	165.3 ± 4.5	1.63 ± 0.12	2.32 ± 0.02	1.80 ± 0.01
T – 210 °C	148.9 ± 4.3	2.27 ± 0.25	2.32 ± 0.01	1.82 ± 0.01
$Ge_{15}Se_{75}$				
as-prepared	236.0 ± 4.0	4.83 ± 0.11	2.03 ± 0.01	1.80 ± 0.01
T – 90 °C	212.2 ± 4.7	4.25 ± 0.26	2.11 ± 0.01	1.75 ± 0.01
T – 120 °C	176.5 ± 6.4	6.93 ± 0.40	2.26 ± 0.01	1.70 ± 0.01
T – 150 °C	156.9 ± 3.0	1.85 ± 0.38	2.38 ± 0.01	1.69 ± 0.01
T – 180 °C	149.2 ± 3.0	0.95 ± 0.15	2.39 ± 0.02	1.71 ± 0.01

for retaining low surface roughness during thermal stabilization and can subsequently achieve a higher optical quality of stabilized ChG thin film.

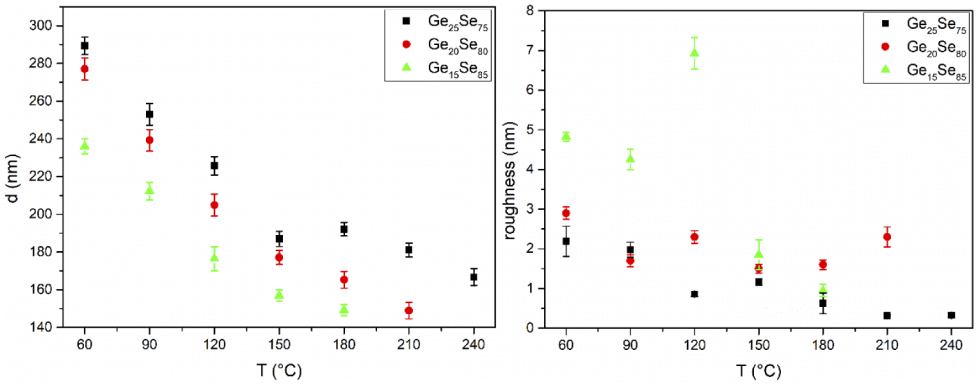

Fig. 3. Thickness (left) and surface roughness (right) of solution processed $Ge_{25}Se_{75}$, $Ge_{20}Se_{80}$ and $Ge_{15}Se_{85}$ thin films.

Refractive index of studied Ge-Se thin films is gradually increasing with increasing annealing temperature up to 150 °C (Fig. 4 - left). Annealing at above 150 °C does not significantly increase the refractive index of thermally stabilized Ge-Se thin films. The data also shows that refractive index of studied Ge-Se thin films is increasing with increasing content of selenium, which is consistent with compositional dependencies obtained by other authors [35,36].

Optical Materials EXPRESS

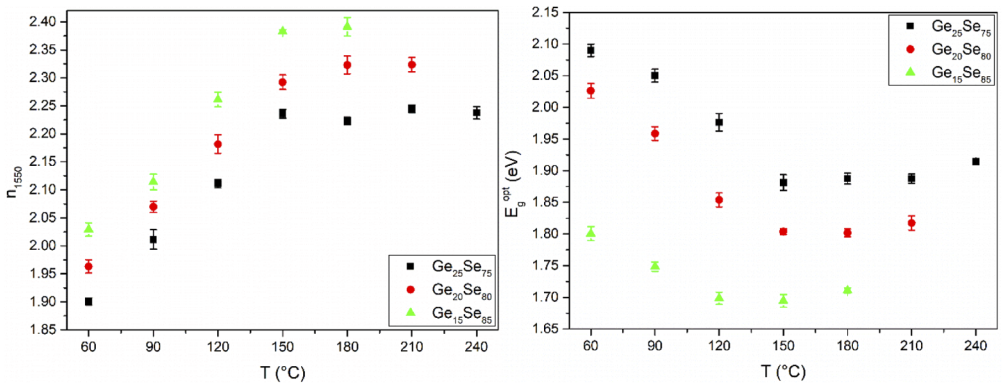

Fig. 4. Refractive index at $\lambda = 1550$ nm (left) and optical bandgap (right) of solution processed $Ge_{25}Se_{75}$, $Ge_{20}Se_{80}$ and $Ge_{15}Se_{85}$ thin films.

Similar trends can be observed in behaviour of optical bandgaps (Fig. 4 - right). Their values are significantly decreasing with increasing annealing temperature up to 150 °C (red shift of short wavelength absorption edge) and thermal stabilization at higher temperatures doesn't result in change of optical bandgaps. There is again a strong compositional dependence as the optical bandgap values are consistently decreasing with increasing content of selenium. Based on obtained findings, there is a strong implication that the most important structural changes in Ge-Se thin film matrix occurs below 150 °C. The temperature range of these changes is independent on composition and T_g of annealed thin film and thus it probably indicates the general range in which the most of Ge-Se dissolution products are decomposed.

Similarly, to previous results with Ge-Sb-S system [15], the optical parameters of solution-processed Ge-Se thin films are different from properties of thin films deposited by conventional vacuum deposition techniques [37–39]. Generally, the refractive indices and optical bandgaps of the Ge-Se thermally stabilized solution processed thin film are lower (e.g. for as-prepared thermally evaporated $Ge_{25}Se_{75}$ thin films n = 2.37 and $E_g{}^{opt} = 2.25$ eV [37]). This can be explained by an expected different structure of both materials (vacuum deposited Ge-Se thin films are often significantly more disordered) despite undergoing thermal stabilization, the solution processed thin films still contain some minor amounts of organic residuals.

The elemental composition of studied solution processed Ge-Se thin films was analysed by EDS technique. The data confirmed that the targeted compositions of thermally stabilized Ge-Se thin films were maintained in almost whole used temperature range (Fig. 5). The exceptions were the highest annealing temperatures for each composition – i.e. 240 °C for $Ge_{25}Se_{75}$ thin films, 210 °C for $Ge_{20}Se_{80}$ thin films and 180 °C for $Ge_{15}Se_{85}$ thin films. There is a clear drop in selenium content, which indicates that the samples reached the temperatures where some part of selenium evaporates from thin film matrix. Such process is in nature undesirable and signifies that thin films of given composition should be annealed only at lower temperatures to avoid selenium loss.

The total nitrogen and oxygen content in matrix of solution processed Ge-Se thin films is depicted in Fig. 6. The nitrogen content represents the content of $PrNH_2$ solvent residuals (occluded and chemically bonded) but we also expect that some small part of the signal can be attributed to molecular N_2 since thin film were deposited in pure nitrogen atmosphere. The oxygen content represents the content of MeOH solvent residual because there is no other expected source of oxygen due to the preparation of thin films in nitrogen filled glovebox (O_2, $H_2O < 0.1$ ppm) and immediate EDS analysis (in vacuum) after removal of prepared thin films from protecting inert atmosphere. The data shows that nitrogen content is strongly dependent on

Optical Materials EXPRESS

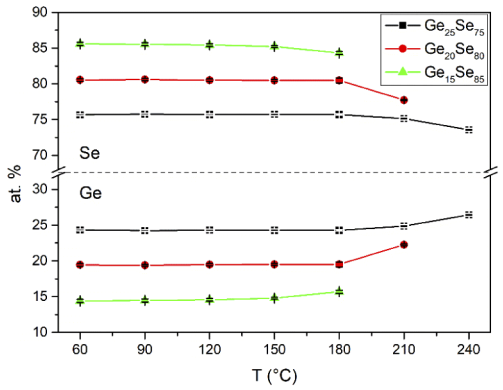

Fig. 5. The elemental composition of solution processed $Ge_{25}Se_{75}$, $Ge_{20}Se_{80}$ and $Ge_{15}Se_{85}$ thin films.

germanium content while oxygen content is practically independent on composition of thin film. This suggests that the most of residual $PrNH_2$ molecules are bonded to germanium (based on dissolution mechanism proposed by [12]) while most of MeOH is probably only trapped in thin film matrix. This confirms the idea that MeOH primarily helps to disperse Ge-Se dissolution products since the MeOH is significantly more polar than $PrNH_2$ alone [21].

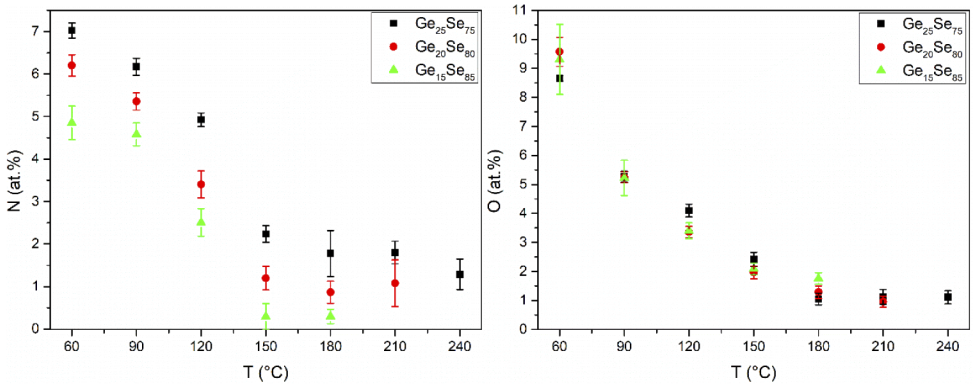

Fig. 6. The total nitrogen (left) and oxygen (right) content in solution processed $Ge_{25}Se_{75}$, $Ge_{20}Se_{80}$ and $Ge_{15}Se_{85}$ thin films.

The content of organic residuals was also studied by FT-IR spectroscopy (Fig. 7). The most dominant bands are located between 2700-3300 cm^{-1}, which can be attributed to the symmetric and asymmetric vibrations of CH_2 and CH_3 groups from $PrNH_2$ and MeOH solvent residuals [40–43]. The wide shoulder between 3300-3600 cm^{-1} belongs to the vibrations of symmetric and asymmetric N-H stretching vibrations of amine groups [40–42] and O-H stretching vibrations of alcohol groups [43]. The weaker bands at 1380 and 1465 cm^{-1} can be attributed to the C-H bending vibrations (C-H methyl rocking and C-H scissoring vibrations, respectively [40–43]). The band at 1575 cm^{-1} belongs to the N-H bending vibrations [40–42]. Increasing annealing temperature is reflected in decreasing intensities of discussed bands as organic residual molecules are leaving thin films matrix. The most significant drop can be observed between 120 and 150 °C, similarly to nitrogen content by EDS at Fig. 6 – left. The data also confirms that despite reaching temperatures, where the Se starts to evaporate (see Fig. 5), the organic residual cannot

Optical Materials EXPRESS

be completely removed from thin films matrix. Similar behaviour was found in other solution processed ChG systems [15,34,44].

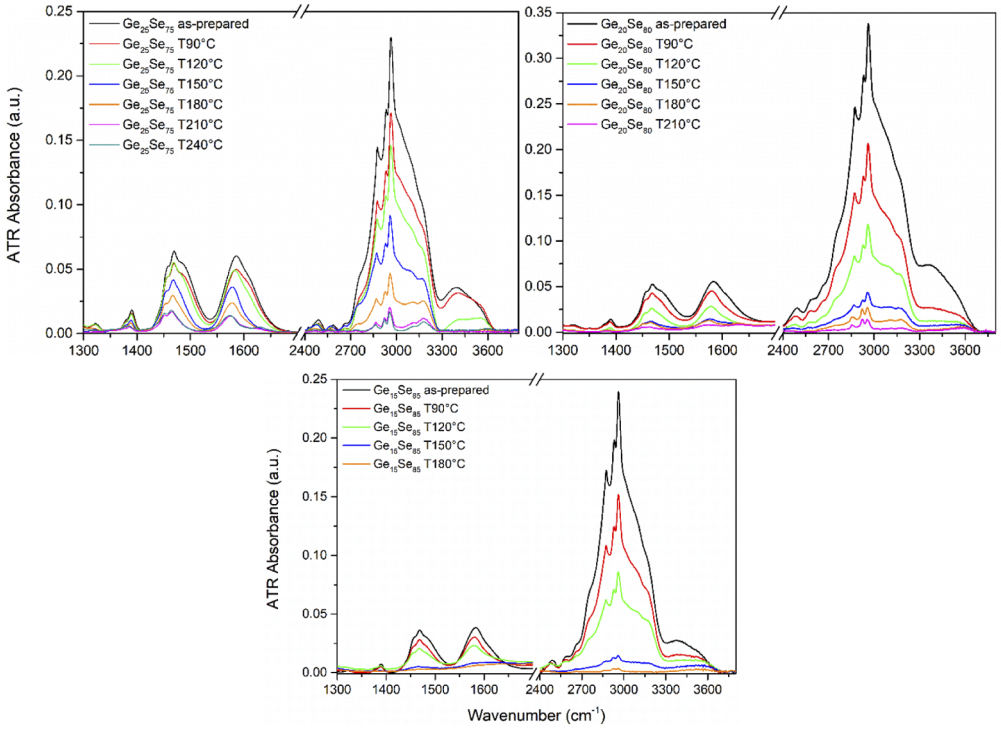

Fig. 7. FT-IR ATR spectra of solution processed $Ge_{25}Se_{75}$, $Ge_{20}Se_{80}$ and $Ge_{15}Se_{85}$ thin films.

The surface of studied Ge-Se solution processed thin films was also analysed by SEM. Images of as-prepared thin films, thin films annealed at maximum used temperature and at temperature 30 °C lower (i.e. at temperature where no significant changes of targeted composition were observed) are given in Fig. 8. The data show that the surface of as-prepared $Ge_{25}Se_{75}$ and $Ge_{20}Se_{80}$ thin films is very smooth without presence of any surface defects. Increasing annealing temperature has no impact on the surface topography of $Ge_{25}Se_{75}$ and $Ge_{20}Se_{80}$ thin films until the maximum used stabilization temperatures are reached (240 °C for $Ge_{25}Se_{75}$ and 210 °C $Ge_{20}Se_{80}$ thin films). The surface starts to be more porous and granular which can be connected with observed loss of Se content (see Fig. 5). Contrary, the surface of as-prepared $Ge_{15}Se_{85}$ thin films is much rougher which is also reflected in observed higher surface roughness by AFM (Fig. 3 – right). Higher surface roughness of as-prepared $Ge_{15}Se_{85}$ thin films probably originates from lower solubility of selenium and selenium-rich compounds in used solvent. Solvent evaporation during thin films deposition forces quick formation of bigger particles of ChG material, which in return forms much rougher surface. However, increasing annealing temperature (and especially annealing above T_g of $Ge_{15}Se_{85}$ ChG material) has positive effect on surface quality, probably due to surface diffusion of ChG material. Similarly to $Ge_{25}Se_{75}$ and $Ge_{20}Se_{80}$ thin films, the annealing at higher temperatures (180 °C for $Ge_{15}Se_{85}$ thin films) forces selenium to evaporates and new surface defects can be observed on stabilized thin films.

The structure of source bulk glasses and deposited Ge-Se thin films was studied by Raman spectroscopy (Fig. 9). The main structural units of $Ge_{25}Se_{75}$ bulk glass are $GeSe_4$ tetrahedrons with the bands at 199 (corner sharing) and 216 cm^{-1} (edge sharing) [45–48]. The next distinctive

Optical Materials EXPRESS

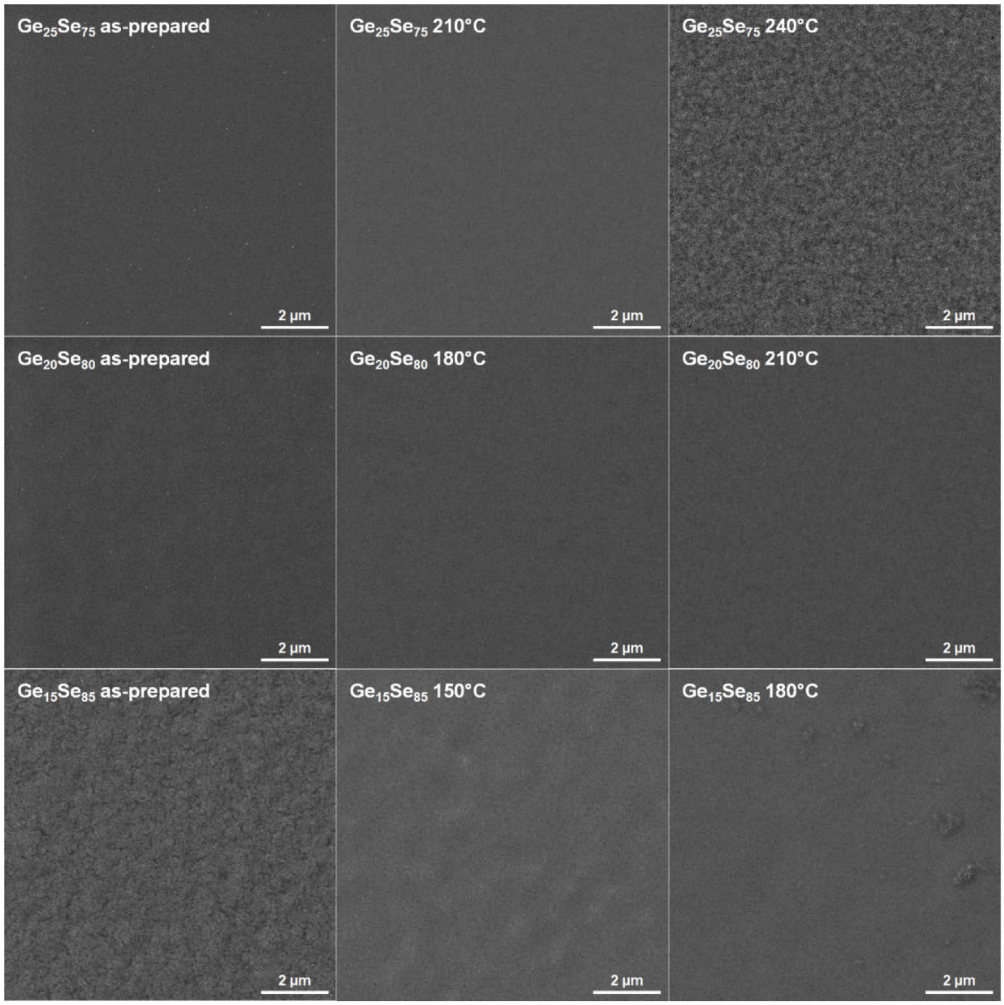

Fig. 8. SEM scans of solution processed $Ge_{25}Se_{75}$, $Ge_{20}Se_{80}$ and $Ge_{15}Se_{85}$ thin films.

wide band with maximum at 263 cm^{-1} can be attributed to the Se-Se vibrations in Se chains (259 cm^{-1}) and at higher frequencies (268 cm^{-1}) to Se_n rings [45–47,49]. The wide band between 70-150 cm^{-1} is related to unresolved lattice modes [46].

The structure of as-prepared $Ge_{25}Se_{75}$ thin film is very different from the structure of source bulk glass. The most dominant band is now located at 253 cm^{-1}. Distinctive shoulder around 235 cm^{-1} and new band at 110 cm^{-1} can be also identified in measured Raman spectrum. All these bands belong to the vibrations of amorphous selenium (dot line in Fig. 9) with distorted ring network structure [50,51]. Similar selenium bands were also found in Raman spectra of As-Se glasses with substantial selenium overstoichiometry [52]. The band of corner shared $GeSe_4$ tetrahedrons at 199 cm^{-1} is also present in Raman spectrum, however its intensity is significantly lower than the band of distorted amorphous selenium rings. The new weak band around 325 cm^{-1} can be also identified in the Raman spectrum of as-prepared $Ge_{25}Se_{75}$ thin film but it hasn't been yet described in literature. Because of its absence in the spectrum of $Ge_{25}Se_{75}$ bulk glass it probably belongs to the vibrations of various Ge-Se dissolution products (similarly to the bands of dissolution products identified in the Raman spectra of soft-baked

Optical Materials EXPRESS

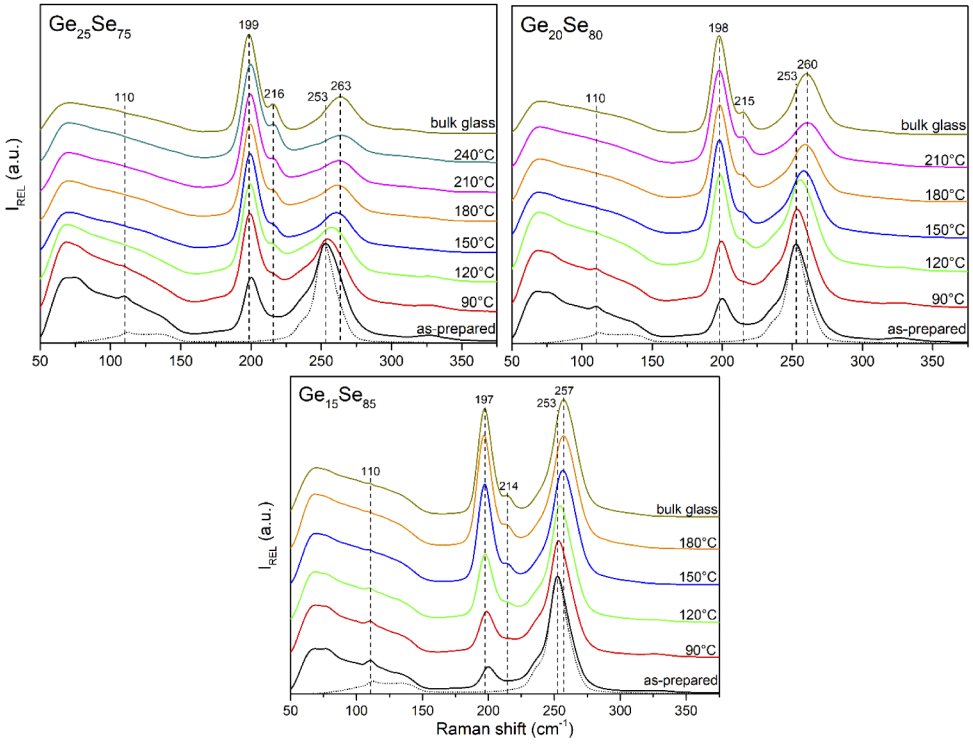

Fig. 9. Raman spectra of source bulk glasses and solution processed $Ge_{25}Se_{75}$, $Ge_{20}Se_{80}$ and $Ge_{15}Se_{85}$ thin films (solid lines) together with Raman spectra of amorphous selenium (dot line).

thin films of As-S and Ge-S system [34,53]). These dissolution products can be described as compounds with organic solvent residuals ($PrNH_2$) bonded to small Ge-Se ChG fragments richer with germanium [54]. The thermal stabilization process induces significant structural changes, which is reflected in shift of the structure of as-prepared thin film towards the structure of source bulk glass. The intensities of $GeSe_4$ corner and edge shared tetrahedrons' bands at 199 and 216 cm^{-1} are increasing with increasing annealing temperature while bands of Ge-Se dissolution products at 325 cm^{-1} and distorted Se rings at 110, 235 and 253 cm^{-1} are decreasing. The frequencies of Se bands are shifting towards their original position in source bulk glass due to the expected thermally induced structural polymerization process, which results in more compact and interlinked ChG structure (as generally observed in all solution processed ChG thin films of other systems). In case of $Ge_{25}Se_{75}$ solution processed thin films, the thermally induced structural changes are practically completed between 150-180 °C. The Raman spectrum of the sample annealed at 240 °C shows sudden decrease of band at 263 cm^{-1} (Se chains and rings), which is consistent with observed decrease of Se content by EDS.

Similar structural features and thermally induced changes can be identified in Raman spectra of $Ge_{20}Se_{80}$ and $Ge_{15}Se_{85}$ source bulk glasses and solution processed thin films. The band of Se chains and rings is gradually getting more dominant with increasing Se content in source bulk glass. The thermal stabilization process is again completed between 150-180 °C and annealing at 210 °C for $Ge_{20}Se_{80}$ thin films and at 180 °C for $Ge_{15}Se_{85}$ thin films induces notable decrease in intensity of Se chains and Se rings band.

The emphasis must be also put on relation of suitable thermal stabilization temperature (150-180 °C) and the T_g of annealed material. For $Ge_{25}Se_{75}$ thin films, the ChG material is stabilized

Optical Materials EXPRESS

quite below T_g of source bulk glass (214-228 °C [30–32]) while for $Ge_{20}Se_{80}$ and $Ge_{15}Se_{85}$ thin films it is stabilized at/or slightly above their T_g ($Ge_{20}Se_{80}$ = 154-159 °C, $Ge_{15}Se_{85}$ = 108-122 °C [30–32]). This confirms that temperature of 150 °C is necessary for thermal decomposition of Ge-Se dissolution products independently on the composition of annealed Ge-Se thin film and subsequently on relaxation and plasticity of Ge-Se ChG matrix. This can potentially cause problems with optical quality of solution processed ChG thin films with higher Se content (more than 85 at. %), because the temperature for decomposition of Ge-Se dissolution products would be eventually higher than the temperature when thin films composition and surface roughness could be compromised (as seen on SEM scans at Fig. 8). On the other hand, we can only speculate about the lowest possible Se content for which multi-component MeOH-$PrNH_2$ solvent approach could be applied. However, based on the T_g of Ge-Se ChGs [31,32] and the results with solution processing in other studied ChG systems [12,20,24,44] we expect that thermally stabilized solution processed thin films with high optical quality and targeted Ge/Se ratio could be prepared at least up to stoichiometric $Ge_{33}Se_{67}$ composition.

The chemical resistance of deposited Ge-Se thin films was studied by wet-etching in EDA based solvent and obtained etching rates are presented in Fig. 10. The as-prepared thin films and thin films annealed at 90 °C were flaked off during wet-etching procedure and corresponding etching rates could not be calculated. The data shows unusual compositional based behaviour in etching rates between 120 and 150 °C. The chemical resistance grows with increasing content of selenium at 120 °C, but when thin films are stabilized at 150 °C the chemical resistance to EDA based solvent revers. It can be explained by significant thermal dependent structural differences of individual solution processed Ge-Se thin films and nature of EDA interaction with etched material. As confirmed by Raman spectroscopy, the thin films annealed below 150 °C (and especially as-prepared thin films) possess the structure rich with dissolution product units and, in this case more importantly, the distorted selenium rings. These selenium based structural units are notoriously very difficult to dissolve in amines alone, which would explain the higher chemical resistance of thin films with more selenium content in composition. As discussed above, the structure of Ge-Se solution processed thin films gets progressively more polymerized with increasing annealing temperature, which is reflected in lower content of insoluble species with Se-Se homopolar bonds. Thus, when the temperature of 150 °C is reached, the structure of annealed thin film is significantly more polymerized and closer to the structure of source bulk glass. The EDA based etching solvent can interact with Ge-Se matrix by usual combination of nucleophilic substitution and possible chelation based dissolution mechanism (similarly to As-S ChGs thin films [12,55]) and films with higher content of germanium are etched slower.

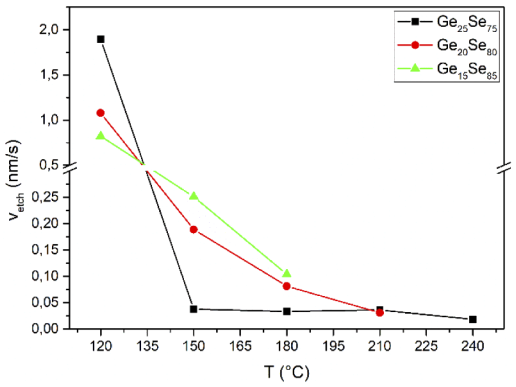

Fig. 10. Etching rates of solution processed $Ge_{25}Se_{75}$, $Ge_{20}Se_{80}$ and $Ge_{15}Se_{85}$ thin films.

Optical Materials EXPRESS

4. Conclusions

The $Ge_{25}Se_{75}$, $Ge_{20}Se_{80}$ and $Ge_{15}Se_{85}$ bulk glasses were quantitatively dissolved in MeOH-$PrNH_2$ solvent mixture. The Ge-Se thin films of all compositions were deposited in high optical quality by spin-coating technique and thermally stabilized to reduce content of organic residuals and polymerize ChG structure. It was found that suitable annealing temperatures (based on changes in structure, composition, chemical resistance and surface roughness) were 150 °C for $Ge_{15}Se_{85}$, 180 °C for $Ge_{20}Se_{80}$ and 210 °C for $Ge_{25}Se_{75}$ thin films (with respect to chosen experimental temperature increments). The stabilized thin films possessed high refractive index (increasing with increasing selenium content), low surface roughness (below 2 nm), targeted elemental composition, significantly reduced content of organic residuals and structure close to source bulk glass. The wet etching of studied Ge-Se thin films proved significant increase of chemical resistance with increasing annealing temperature and compositional dependant etching rate.

Funding

Ministerstvo Školství, Mládeže a Tělovýchovy (LM2018103); European Regional Development Fund (CZ.02.1.01/0.0/0.0/17_048/0007376).

Disclosures

The authors declare no conflicts of interest.

References

1. J.-L. Adam and X. Zhang, *Chalcogenide Glasses: Preparation, Properties and Applications* (Woodhead Publishing, 2014).
2. K. Tanaka and K. Shimakawa, *Amorphous Chalcogenide Semiconductors and Related Materials* (Springer, 2011).
3. S. Song, S. S. Howard, Z. Liu, A. O. Dirisu, C. F. Gmachl, and C. B. Arnold, "Mode tuning of quantum cascade lasers through optical processing of chalcogenide glass claddings," Appl. Phys. Lett. **89**(4), 041115 (2006).
4. Z. Borisova, *Glassy Semiconductors* (Plenum Press, 1981).
5. D. H. Cha, H.-J. Kim, Y. Hwang, J. C. Jeong, and J.-H. Kim, "Fabrication of molded chalcogenide-glass lens for thermal imaging applications," Appl. Opt. **51**(23), 5649–5656 (2012).
6. D. H. Cha, Y. Hwang, J.-H. Kim, D.-S. Kim, and H.-J. Kim, "Fabrication of chalcogenide glass lens module for thermal security camera," Proc. SPIE **9249**, 924916 (2014).
7. A. V. Rode, A. Zakery, M. Samoc, R. P. Charters, E. G. Gamaly, and B. Luther- Davies, "Laser-deposited As_2S_3 chalcogenide films for waveguide applications," Appl. Surf. Sci. **197-198**, 481–485 (2002).
8. A. Zoubir, M. Richardson, C. Rivero, A. Schulte, C. Lopez, K. Richardson, N. Hô, and R. Vallee, "Direct femtosecond laser writing of waveguides in As_2S_3 thin films," Opt. Lett. **29**(7), 748–750 (2004).
9. G. Lucovsky and J. Philips, "Reversible chemical phase separation in on-state of art ReWritable (RW) $Ge_2Sb_2Te_5$ optical phase change memories," J. Non-Cryst. Solids **354**(19-25), 2753–2756 (2008).
10. H. Jain and M. Vlcek, "Glasses for lithography," J. Non-Cryst. Solids **354**(12-13), 1401–1406 (2008).
11. R. M. Almeida, L. F. Santos, A. Simens, A. Ganjoo, and H. Jain, "Structural heterogeneity in chalcogenide glass films prepared by thermal evaporation," J. Non-Cryst. Solids **353**(18-21), 2066–2068 (2007).
12. G. C. Cherna and I. Lauks, "Spin coated amorphous chalcogenide films," J. Appl. Phys. **53**(10), 6979–6982 (1982).
13. S. Novak, D. E. Johnston, C. Li, W. Deng, and K. Richardson, "Deposition of $Ge_{23}Sb_7S_{70}$ chalcogenide glass films by electrospray," Thin Solid Films **588**, 56–60 (2015).
14. K. Palka, T. Syrovy, S. Schröter, S. Brückner, M. Rothhardt, and M. Vlcek, "Preparation of arsenic sulfide thin films for integrated optical elements by spiral bar coating," Opt. Mater. Express **4**(2), 384–395 (2014).
15. S. Slang, P. Janicek, K. Palka, L. Loghina, and M. Vlcek, "Optical properties and surface structuring of $Ge_{20}Sb_5S_{75}$ amorphous chalcogenide thin films deposited by spin-coating and vacuum thermal evaporation," Mater. Chem. Phys. **203**, 310–318 (2018).
16. S. Novak, L. Scarpantonio, J. Novak, M. D. Pre, A. Martucci, J. D. Musgraves, N. D. McClenaghan, and K. Richardson, "Incorporation of luminescent CdSe/ZnS core-shell quantum dots and PbS quantum dots into solution-derived chalcogenide glass films," Opt. Mater. Express **3**(6), 729–738 (2013).
17. S. Slang, P. Janicek, K. Palka, and M. Vlcek, "Solution processed $Ge_{20}Sb_5S_{75}$ thin films: the effect of solution concentration and multiple layers stacking," Opt. Mater. Express **9**(11), 4360–4369 (2019).
18. S. Slang, L. Loghina, K. Palka, and M. Vlcek, "Exposure enhanced photoluminescence of $CdS_{0.9}Se_{0.1}$ quantum dots embedded in spincoated $Ge_{25}S_{75}$ thin films," RSC Adv. **7**(85), 53830–53838 (2017).

Optical Materials EXPRESS

19. T. Kohoutek, T. Wagner, M. Frumar, A. Chrissanthopoulos, O. Kostadinova, and S. N. Yannopoulos, "Effect of cluster size of chalcogenide glass nanocolloidal solutions on the surface morphology of spin-coated amorphous films," J. Appl. Phys. **103**(6), 063511 (2008).
20. S. Song, J. Dua, and C. B. Arnold, "Influence of annealing conditions on the optical and structural properties of spin-coated As_2S_3 chalcogenide glass thin films," Opt. Mater. Express **18**(6), 5472–5480 (2010).
21. S. Slang, K. Palka, P. Janicek, M. Grinco, and M. Vlcek, "Solution processed $As_{30}Se_{70}$ chalcogenide glass thin films with specular optical quality: multi-component solvent approach," Opt. Mater. Express **8**(4), 948–959 (2018).
22. S. M. R. Ullah, A. A. Simon, and M. Mitkova, "Studies and Analysis of Ge_xSe_{100-x} Based Spin Coated Chalcogenide Thin Films," Microsc. Microanal. **25**(S2), 2608–2609 (2019).
23. I. Sebastian, S. Divya, V. P. N. Nampoori, P. Radhakrishnan, and S. Thomas, "Impact of intermediate localized states on nonlinear optical absorption of Ga-Ge-Se nanocolloidal solutions," Appl. Phys. Lett. **102**(3), 031115 (2013).
24. D. H. Webber and R. L. Brutchey, "Alkahest for V_2VI_3 Chalcogenides: Dissolution of Nine Bulk Semiconductors in a Diamine-Dithiol Solvent Mixture," J. Am. Chem. Soc. **135**(42), 15722–15725 (2013).
25. K. Palka, S. Slang, J. Buzek, and M. Vlcek, "Selective etching of spin-coated and thermally evaporated $As_{30}S_{45}Se_{25}$ thin films," J. Non-Cryst. Solids **447**, 104–109 (2016).
26. S. H. Wemple and M. DiDomenico, "Behavior of the Electronic Dielectric Constant in Covalent and Ionic Materials," Phys. Rev. B **3**(4), 1338–1351 (1971).
27. R. Swanepoel, "Determination of the thickness and optical constants of amorphous silicon," J. Phys. E: Sci. Instrum. **16**(12), 1214–1222 (1983).
28. J. Tauc, "Absorption edge and internal electric fields in amorphous semiconductors," Mater. Res. Bull. **5**(8), 721–729 (1970).
29. L. Loghina, K. Palka, J. Buzek, S. Slang, and M. Vlcek, "Selective wet etching of amorphous As_2Se_3 thin films," J. Non-Cryst. Solids **430**, 21–24 (2015).
30. P. J. Webber and J. A. Savage, "Some physical properties of Ge-As-Se infrared optical glasses," J. Non-Cryst. Solids **20**(2), 271–283 (1976).
31. J.-P. Guin, T. Rouxel, V. Keryvin, J.-C. Sangleboeuf, I. Serre, and J. Lucas, "Indentation creep of Ge–Se chalcogenide glasses below T_g: elastic recovery and non-Newtonian flow," J. Non-Cryst. Solids **298**(2-3), 260–269 (2002).
32. U. Senapati and A. K. Varshneya, "Viscosity of chalcogenide glass-forming liquids: an anomaly in the 'strong' and 'fragile' classification," J. Non-Cryst. Solids **197**(2-3), 210–218 (1996).
33. Y. Liu, J. Wu, G. Yang, T. Zhao, and S. Shi, "Predicting the onset temperature (T_g) of Ge_xSe_{1-x} glass transition: a feature selection based two-stage support vector regression method," Sci. Bull. **64**(16), 1195–1203 (2019).
34. S. Slang, P. Janicek, K. Palka, and M. Vlcek, "Structure and properties of spin-coated $Ge_{25}S_{75}$ chalcogenide thin films," Opt. Mater. Express **6**(6), 1973–1985 (2016).
35. T. T. Nang, M. Okuda, and T. Matsushita, "Compositional dependenace of the refractive index and its photo-induced variation in the binary glasses systems: $Ge_{1-x}Se_x$ and $As_{1-x}Se_x$," J. Non-Cryst. Solids **33**(3), 311–323 (1979).
36. J. Orava, T. Kohoutek, T. Wagner, Z. Cerna, M. Vlcek, L. Benes, B. Frumarova, and M. Frumar, "Optical and structural properties of Ge–Se bulk glasses and Ag–Ge–Se thin films," J. Non-Cryst. Solids **355**(37-42), 1951–1954 (2009).
37. L. Tichy, H. Ticha, P. Nagels, and R. Callaerts, "Photoinduced optical changes in amorphous Se and Ge-Se films," J. Non-Cryst. Solids **240**(1-3), 177–181 (1998).
38. R. K. Pan, H. Z. Tao, J. Z. Wang, J. Y. Wang, H. F. Chu, T. J. Zhang, D. F. Wang, and X. J. Zhao, "Structure and optical properties of amorphous Ge–Se films prepared by pulsed laser deposition," Optik **124**(21), 4943–4946 (2013).
39. M. Dongol, A. F. Elhady, M. S. Ebied, and A. A. Abuelwafa, "Impact of sulfur content on structural and optical properties of $Ge_{20}Se_{80-x}S_x$ chalcogenide glasses thin films," Opt. Mater. **78**, 266–272 (2018).
40. P. Espeel, F. Goethals, F. Driessen, L. T. Nguyen, and F. E. Du Prez, "One-pot, additive-free preparation of functionalized polyurethanes viaamine–thiol–ene conjugation," Polym. Chem. **4**(8), 2449–2456 (2013).
41. V. T. Liveri, D. Lombardo, M. Pochylski, and P. Calandra, "Molecular association of small amphiphiles: Origin of ionic liquid properties in dibutyl phosphate/propylamine binary mixtures," J. Mol. Liq. **263**, 274–281 (2018).
42. O. Alver, C. Parlak, and M. Senyel, "Theoretical and experimental vibrational spectroscopic study of 3-piperidino-propylamine," J. Mol. Struct. **923**(1-3), 120–126 (2009).
43. D. S. Bulgarevich, Y. Horikawa, and T. Sako, "ATR FT-IR studies of supercritical methanol," J. Supercrit. Fluids **46**(2), 206–210 (2008).
44. G. C. Chern, I. Lauks, and A. R. McGhie, "Spin coated amorphous chalcogenide films: Thermal properties," J. Appl. Phys. **54**(8), 4596–4601 (1983).
45. R. Holomb, V. Mitsa, E. Akalin, S. Akyuz, and M. Sichta, "Ab initio and Raman study of medium range ordering in $GeSe_2$ glass," J. Non-Cryst. Solids **373-374**, 51–56 (2013).
46. R. K. Pan, H. Z. Tao, H. C. Zang, X. J. Zhao, and T. J. Zhang, "Annealing effects on the structure and optical properties of $GeSe_2$ and $GeSe_4$ films prepared by PLD," J. Alloys Compd. **484**(1-2), 645–648 (2009).
47. C. Jiang, X. Wang, Q. Zhu, Q. Nie, M. Zhu, P. Zhang, S. Dai, X. Shen, T. Xu, C. Cheng, F. Liao, Z. Liu, and X. Zhang, "Improvements on the optical properties of Ge–Sb–Se chalcogenide glasses with iodine incorporation," Infrared Phys. Technol. **73**, 54–61 (2015).
48. M. Mitkova, Y. Wang, and P. Boolchand, "Dual Chemical Role of Ag as an Additive in Chalcogenide Glasses," Phys. Rev. Lett. **83**(19), 3848–3851 (1999).

Optical Materials EXPRESS

49. V. V. Poborchii, A. V. Kolobov, J. Caro, V. V. Zhuravlev, and K. Tanaka, "Polarized Raman spectra of selenium species confined in nanochannels of AlPO-5 single crystals," Chem. Phys. Lett. **280**(1-2), 17–23 (1997).
50. A. H. Goldan, C. Li, S. J. Pennycook, J. Schneider, A. Blom, and W. Zhao, "Molecular structure of vapor-deposited amorphous selenium," J. Appl. Phys. **120**(13), 135101 (2016).
51. K. Nagata, T. Ishikawa, and Y. Miyamoto, "Raman spectrum of selenium dissolved in an aqueous solution of sodium sulphide," Jpn. J. Appl. Phys. **24**(Part 1, No. 9), 1171–1173 (1985).
52. V. I. Mikla and V. V. Mikla, "Structural transformations in amorphous As_xSe_{1-X} ($0 \le x \le 0.20$) films," Mol. Phys. **106**(16-18), 2053–2076 (2008).
53. S. Slang, K. Palka, L. Loghina, A. Kovalskiy, H. Jain, and M. Vlcek, "Mechanism of the dissolution of As–S chalcogenide glass in n-butylamine and its influence on the structure of spin coated layers," J. Non-Cryst. Solids **426**, 125–131 (2015).
54. M. Waldman, J. D. Musgraves, K. Richardson, and C. B. Arnold, "Structural properties of solution processed $Ge_{23}Sb_7S_{70}$ glass materials," J. Mater. Chem. **22**(34), 17848–175852 (2012).
55. T. A. Guiton and C. G. Pantano, "Solution/Gelation of Arsenic Trisulfide in Amine Solvents," Chem. Mater. **1**(5), 558–563 (1989).